

## YOUNG'S MODULUS OF PREFIRED QUARTZ PORCELAIN IN A TEMPERATURE RANGE OF 20–1200 °C

### YOUNGOV MODUL PREDŽGANEGA KREMENOVEGA PORCELANA V TEMPERATURNEM OBMOČJU MED 20 °C IN 1200 °C

Anton Trník<sup>1,2\*</sup>, Igor Štubňa<sup>1</sup>, Ján Ondruška<sup>1</sup>, Peter Šín<sup>3</sup>, Štefan Csáki<sup>4</sup>

<sup>1</sup>Constantine the Philosopher University in Nitra, Faculty of Natural Sciences, Department of Physics, Tr. A. Hlinku 1, 94974 Nitra, Slovakia

<sup>2</sup>Czech Technical University Prague, Faculty of Civil Engineering, Department of Materials Engineering and Chemistry, Thakurova 7, 16629 Prague, Czech Republic

<sup>3</sup>Slovak University of Technology in Nitra, Faculty of Civil Engineering, Department of Physics, Radlinského 11, 81005 Bratislava, Slovakia

<sup>4</sup>Czech Academy of Sciences, Institute of Plasma Physics, Za Slovákovou 3, 18200 Prague, Czech Republic

Prejem rokopisa – received: 2018-11-22; sprejem za objavo – accepted for publication: 2019-02-25

doi:10.17222/mit.2018.252

Green samples (50 w% of kaolin, 25 w% of quartz and 25 w% of feldspar) are prefired up to 400–1200 °C and analyzed during their second firing. Thermogravimetry, thermodilatometry and dynamic thermomechanical analyses are performed in a range from room temperature to 1100 °C. In the samples prefired at temperatures of up to 400 °C and 500 °C, the release of physically bound water has a significant influence on Young's modulus, increasing its values by ≈25 % and 6.5 %, respectively, between room temperature and 200 °C. In the samples prefired at temperatures above 500 °C, the  $\alpha \rightarrow \beta$  transition of quartz governs Young's modulus in a temperature interval of 500–700 °C. Young's modulus increases by 29–40 % in the samples prefired at 600–1200 °C due to the closing of the cracks located around quartz grains. The presence of a glassy phase is not necessary for the steep increase of Young's modulus around the  $\alpha \rightarrow \beta$  transition of quartz. At high temperatures, an increase in Young's modulus is caused by solid-phase sintering (above 800 °C), formation of Al-Si spinel ( $\approx 950$ –980 °C) and crystallization of mullite (above 1050 °C).

Keywords: mechanical properties, Young's modulus, porcelain, firing, non-destructive evaluation

Avtorji prispevka so surovce iz 50 masnih % kaolina, 25 masnih % kremenjaka in 25 masnih % živca oz. ortoklaza predžgali na temperaturah od 400 do 1200 °C in jih analizirali med drugim žganjem (sintranjem). Izvedli so termogravimetrične, termodilatometrične in termomehanske analize pri temperaturah od sobne temperature do 1100 °C. V predžganih vzorcih, predžganih na temperaturah do 400 °C in 500 °C, se je sprostila fizikalno vezana voda, kar je imelo pomemben vpliv na Youngov modul. Le-ta je narasel za približno 25 % oz. 6,5 % med sobno temperaturo in 200 °C. Na vzorcih, predžganih nad temperaturo 500 °C, je prišlo do prehoda iz  $\alpha$  v  $\beta$  fazo. Vsebnost kremena določa vrednost Youngovega modula v temperaturnem območju med 500 °C in 700 °C. Youngov modul naraste od 29 % do 40 % v vzorcih predžganih na temperaturah med 600 °C in 1200 °C zaradi zapiranja razpok lociranih med zrni kremena. Prisotnost steklaste faze ni potrebna za nadaljnje povečanje Youngovega modula okoli prehoda iz  $\alpha$  v  $\beta$  kremen. Pri visokih temperaturah je povečanje Youngovega modula posledica sintranja v trdni fazi (nad 800 °C), tvorbe Al-Si špinela (med približno 950 °C in 980 °C) in kristalizacije mulita (nad 1050 °C).

Ključne besede: mehanske lastnosti, Youngov modul, porcelan, žganje, neporušne preiskave

## 1 INTRODUCTION

Mechanical properties of ceramic materials depend on multiple factors such as mineral composition, granulometric distribution, firing regime and others.<sup>1</sup> Particularly Young's modulus, Poisson's ratio and mechanical strength are the most important quantities that determine the utility properties of ceramics from the mechanical point of view. If a fired ceramic mixture contains a sufficient amount of quartz, the relationship between Young's modulus and the temperature measured during the heating reflects the presence of quartz through a steep increase in the values of Young's modulus in a relatively narrow interval around the  $\alpha \rightarrow \beta$  transition of quartz. This was found on quartz porcelain fired at 1320 °C,<sup>2,3</sup> on corundum porcelain fired at 1330 °C,<sup>4</sup> and also on

illite-based tiles fired at 1100 °C and 1200 °C.<sup>5,6</sup> This increase in Young's modulus is caused by the closing of the circumference cracks around the quartz grains.<sup>2,5</sup> The same effect was observed on ceramics including cristobalite. Like quartz, when cristobalite passes through its  $\alpha \rightarrow \beta$  transition at  $\approx 220$  °C, it steeply increases its volume, and the microcracks located around the cristobalite grains are healed, leading to a steep increase in Young's modulus.<sup>7,8</sup> The influence of the  $\alpha \rightarrow \beta$  transition of quartz on Young's modulus was measured on both kaolinite-based and illite-based samples, in which a glassy phase was developed.<sup>2,5</sup>

To reveal these influences, Young's modulus must be measured in-situ during heating using a dynamic thermomechanical analysis (D-TMA) that utilizes the sonic resonant method or impulse excitation technique for measuring the frequency of the resonant vibration of a sample. Thermodilatometry (TDA) and thermogravi-

\*Corresponding author's e-mail:  
atnik@ukf.sk; anton.trnik@fsv.cvut.cz

metry (TG) should be also used to determine the actual dimensions and the mass of the sample and obtain the values of Young's modulus with a sufficient accuracy.<sup>9,10</sup>

In the ceramic technology, particularly in pottery production, two-stage firing is often used. The first stage, the so-called biscuit firing, converts clay into ceramics. The common temperature for biscuit firings of kaolin-quartz-feldspar mixtures is 900–1000 °C. After this firing, a glaze is applied and the products are fired again.<sup>7,11,12</sup> The available literature focused on the biscuit firing, that is, the firing of the green ceramic body.<sup>13–16</sup> Contrary to this, there is very little published research on the processes that take place during the second firing. This research deals with ceramic samples fired at high temperatures, i.e., samples that contain the glassy phase.

The objective of this study is to analyze the second firing of the samples prefired (i.e., biscuit-fired) at temperatures of 400–1200 °C. The samples prefired at 400–1000 °C do not contain the glassy phase. Although only biscuit firings at temperatures of 900–1000 °C have practical applications, we also studied the products prefired at lower temperatures in order to reveal the influences of the release of the physically bound water, dehydroxylation, the  $\alpha \rightarrow \beta$  transition of quartz, solid-phase sintering and high-temperature phase transitions on Young's modulus during the second firing.

## 2 EXPERIMENTAL PART

The green plastic mixture was made from kaolin (50 w%), quartz (25 w%) and feldspar (25 w%) mixed with distilled water. The chemical composition of kaolin and feldspar is given in **Table 1**.

**Table 1:** Chemical composition of Sedlec kaolin and feldspar in mass fractions (w%)

	SiO <sub>2</sub>	Al <sub>2</sub> O <sub>3</sub>	Fe <sub>2</sub> O <sub>3</sub>	TiO <sub>2</sub>	CaO	MgO	K <sub>2</sub> O	Na <sub>2</sub> O	LOI
kaolin	45.8	37.3	1.0	0.2	0.6	0.5	1.2	0.6	12.8
feldspar	70.2	15.2	0.3	0.3	0.5	0.3	10.5	2.1	0.6

Samples were extruded using a laboratory extruder; they had a cylindrical shape with a diameter of 11 mm. After free drying in open air at room temperature for 1 week, 1 % of the mass of these green samples was physically bound water. The sample dimensions were  $\phi 10 \times 140$  mm for the resonant apparatus<sup>10</sup>,  $\phi 10 \times 40$  for the dilatometer<sup>17</sup> and  $\phi 10 \times 20$  for the TG analyzer.<sup>18</sup>

The samples were fired up to the selected temperature (400–1200 °C) with a heating rate of 5 °C·min<sup>-1</sup>, without soaking at the selected temperature and then cooled down to room temperature in a furnace (in the text below, the samples are marked as S400, S500, ... S1200 according to their firing temperature). The samples were stored in air in laboratory conditions. Then the samples were subjected to the D-TMA based on the sonic resonant method, TDA and TG, with the heating rate of 5 °C·min<sup>-1</sup> reaching up to 1100 °C.

Resonant frequency was measured using a D-TMA analyzer, described in detail in reference literature<sup>10</sup>; then Young's modulus was calculated with the formula given by the ASTM standard<sup>19</sup> and rewritten for temperature-dependent quantities and for the cylindrical sample as:

$$E(t) = 1.6774 \frac{m_0 l^3}{d_0^4} \frac{[1 + \Delta m(t)/m_0]}{[1 + \Delta l(t)/l]} f^2(t) \quad (1)$$

where  $\Delta l(t)/l_0$  and  $\Delta m(t)/m_0$  indicate the relative linear thermal expansion and relative mass change of a sample measured with the dilatometer and TG analyzer, respectively. In Equation (1), the equal relative expansions of the sample in the axial and radial directions were presumed. The values for  $l_0$ ,  $d_0$ , and  $m_0$  are the initial length, diameter and mass of the sample at room temperature, respectively, and  $f(t)$  is the resonant frequency of the fundamental mode of the flexural vibration at the temperature  $t$ . Since the ratio  $l_0/d_0 < 20$ , the correction coefficient, calculated in accordance with the ASTM standard,<sup>19</sup> was incorporated into Equation (1).

Since Young's modulus is proportional to the bulk density, it is useful to derive this quantity from the TG and TDA results in accordance with the following Equation (2):

$$\rho(t) = \frac{m_0 [1 + \Delta m(t)/m_0]}{V_0 [1 + 3\Delta l(t)/l_0]} f^2(t) \quad (2)$$

in which  $V_0$  is the volume of the sample at room temperature and other quantities from Equation (2) are described above. The highest biscuit-firing temperature does not exceed 1100 °C; therefore, the maximum experimental firings were performed up to this temperature.

## 3 RESULTS AND DISCUSSION

To obtain the correct value of Young's modulus, the results of the TDA and TG are necessary for Equation (1). Results of  $\Delta l(t)/l_0$  of the prefired samples are depicted in **Figures 1, 2 and 3**. TDA curves for samples S400 and S500 reflect the presence of the physically bound water at the lowest temperatures. The thermal expansion is decelerated by the removal of the water from the pores, causing the crystals to move closer to each other. The dehydroxylation of kaolinite, which starts at  $\approx 450$  °C, is accompanied by a contraction of kaolinite. Based on the dehydroxylation, the  $\alpha \rightarrow \beta$  transition of quartz takes place. The quartz grains increase their volume, which is indicated by small peaks at  $\approx 573$  °C. After the completion of dehydroxylation, an expansion is observed, again up to  $\approx 950$  °C when a collapse of metakaolinite and a formation of Al-Si spinel occur. The compaction, which takes place above 1050 °C, is related to the crystallization of mullite. These phase changes and solid-phase sintering start an intensive contraction.<sup>20</sup> Samples S600 and S700 lose a big

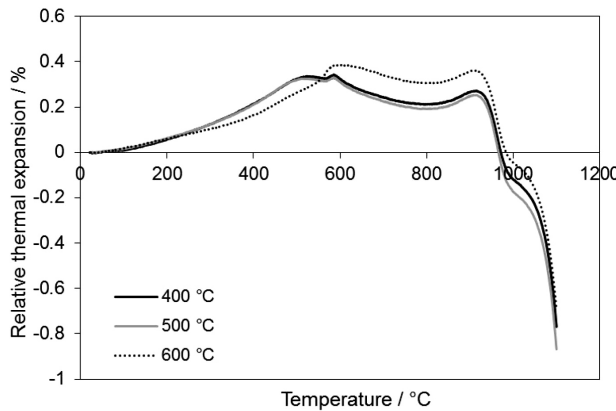


**Figure 1:** Relative thermal expansion of quartz-porcelain samples prefired at (400, 500 and 600) °C

part of their constituent water during the first firing, so the influence of dehydroxylation appears only slightly in the TDA curves; consequently, the  $\alpha \rightarrow \beta$  transition of quartz is indicated as a step at  $\approx 573$  °C. This step is also observed for samples S800, S900, S1000, S1100 and S1200. Sample S1200 contains a glassy phase, which is formed in the kaolinite-quartz-feldspar mixture at temperatures above 1100 °C.<sup>7</sup> The presence of the glassy phase causes a downward bend in the TDA curve, which happens due to the pressure of the dilatometer's rod on the softened sample at high temperatures. We also observe it for sample S1200.

Thermogravimetric curves of samples S400, S500, S600 and S700 (**Figure 4**) show two steps of the mass loss. The first step, which takes place at low temperatures (20–200 °C) is caused by the release of the physically bound water. For the samples prefired at higher temperatures, which are partially sintered, the first step of the mass loss is negligible or missing. The second step, observed between 450 °C and 650 °C, is a consequence of dehydroxylation. This mass loss decreases with the prefiring temperature. Samples S800, S900, S1000, S1100 and S1200 are fully dehydroxylated; so, no second step of the mass loss is registered.

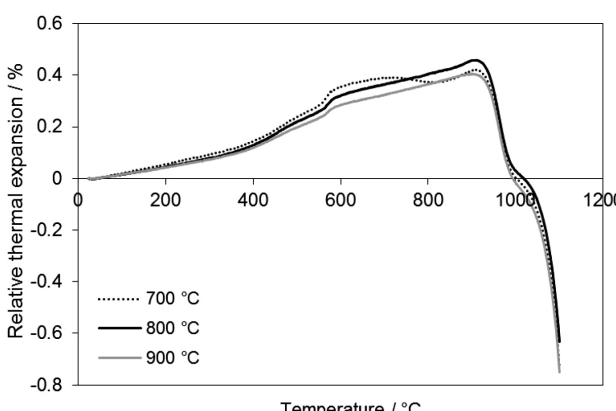


**Figure 2:** Relative thermal expansion of quartz-porcelain samples prefired at (700, 800 and 900) °C

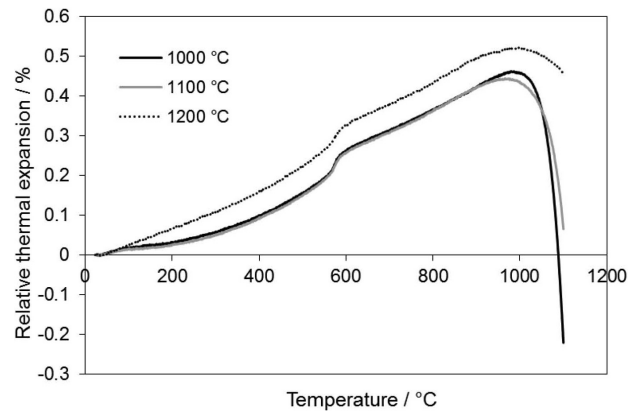


**Figure 3:** Relative thermal expansion of quartz-porcelain samples prefired at (1000, 1100 and 1200) °C

The removal of the physically bound water leads to a decrease in the bulk density at low temperatures. Bulk densities of samples S400, S500 and S600 (**Figure 5**), which are not fully dehydroxylated, have characteristic broad minima as a consequence of the mass loss during the dehydroxylation. Above 900 °C, the bulk density increases due to structural changes and solid-phase sintering. Similar results were obtained for pure kaolin.<sup>21</sup> The changes in the bulk density of samples S700, S800 and S900 (**Figure 6**) as well as samples S1000, S1100 and S1200 (**Figure 7**) are caused only by the thermal expansion because their mass is constant over the whole studied temperature interval. However, this does not apply to sample S700 in the temperature interval from room temperature up to 200 °C where the mass changes during the liberation of the physically bound water (**Figure 4**) also influence its bulk density. The bulk density at high temperatures increases in two steps. The first is due to the collapse of the metakaolinite lattice (at  $\approx 950$  °C) and the second step is due to the creation of mullite (at  $\approx 1050$  °C).

The temperature dependences of Young's modulus of samples S400, S500 and S600 are shown in **Figure 8**. In the temperature interval of 20–200 °C, the values of

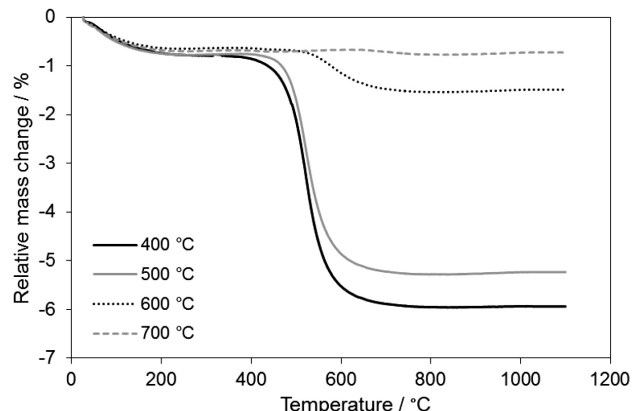


**Figure 4:** Relative mass change of quartz-porcelain samples prefired at (400, 500, 600 and 700) °C

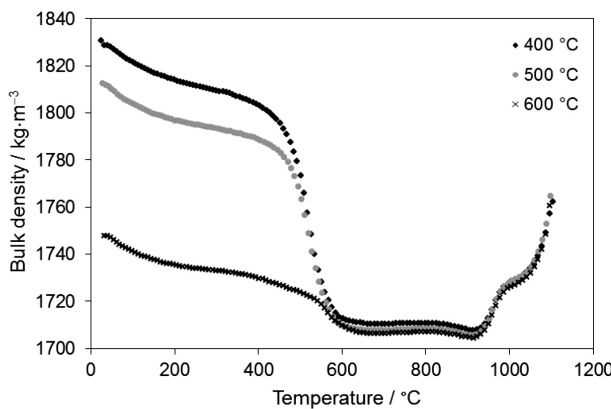


**Figure 5:** Bulk density of quartz-porcelain samples prefired at (400, 500 and 600) °C

Young's modulus increase in accordance with the following rule: the higher the preheating temperature, the lesser is the increase of Young's modulus. For S400, we observe this increase to be  $\approx 23\%$  and for S600 only 2 %. This increase is caused by the removal of the physically bound water from the pores, micropores and crystal surfaces. It leads to tighter contacts between kaolinite crystals, subsequently interfering with the sample expansion. The friction between the crystals and their little jumps during the heating are the source of weak acoustic-emission signals in the green quartz porcelain mixture at temperatures lower than 250 °C.<sup>22</sup> Samples S400, S500 and S600 expand between 20 °C and 200 °C (**Figure 1**), also losing their mass; consequently, their bulk density decreases. In spite of this, Young's modulus increases, which can be explained with the improved contacts between the crystals as no changes take place inside them. Since samples S400, S500 and S600 were completely dried during the preheating, the physically bound water, present in these samples, is the moisture absorbed from air while the samples were being stored in the laboratory.

The next process taking place in samples S400, S500 and S600 during the heating is dehydroxylation of kaolinite. Dehydroxylation leads to microporosity and

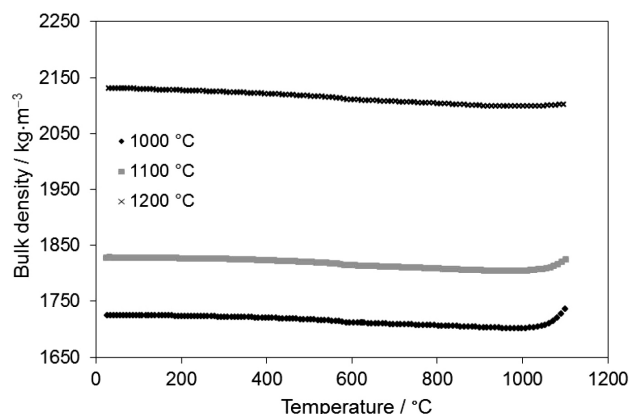


**Figure 7:** Bulk density of quartz-porcelain samples prefired at (1000, 1100 and 1200) °C

defects inside the kaolinite crystals<sup>21,23</sup> and increases the porosity of the quartz-porcelain samples,<sup>7,23,24</sup> i.e., a decrease in Young's modulus should be expected. The decrease was observed for pure kaolin,<sup>25</sup> but not for the quartz-porcelain mixture.<sup>22</sup> The influence of dehydroxylation is visible only for samples S400 and S500 where Young's modulus decreases above 500 °C. Only a little amount of the constituent water remained in sample S600, so no influence of dehydroxylation on Young's modulus is registered. The elastic behavior of the samples that lose their constituent water in the dehydroxylation region has two contrary features. On the one hand, the dehydroxylation is a source of highly defecting metakaolinite crystals<sup>26</sup> that are mechanically weaker than the kaolinite crystals. This leads to a decrease in Young's modulus. On the other hand, dehydroxylation is a source of electrically charged defects. Many of them are supposedly located on the metakaolinite-crystal faces and, consequently, electrostatic forces fortify the sample. This increases Young's modulus. The superposition of these two products of dehydroxylation determines Young's modulus behavior of the kaolin-based samples during their heating between 400 °C and 700 °C.

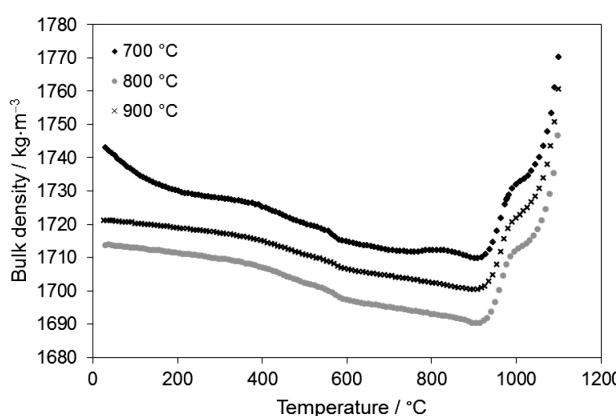


**Figure 6:** Bulk density of quartz-porcelain samples prefired at (700, 800 and 900) °C

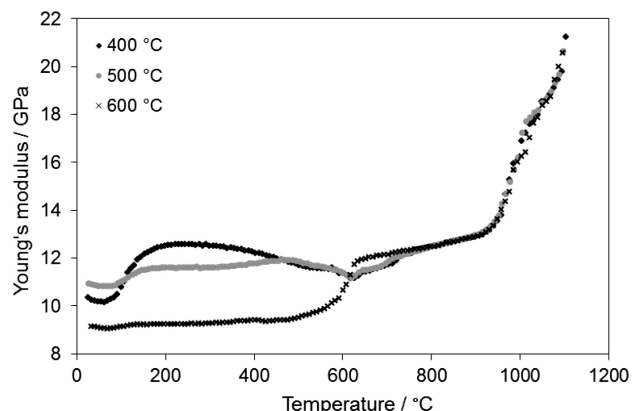


**Figure 8:** Young's modulus of quartz-porcelain samples prefired at (400, 500 and 600) °C

Since the samples contain ≈25 w% of quartz, the  $\alpha \rightarrow \beta$  transition of quartz grains around the temperature of 573 °C, which is accompanied by their volume increase by ≈0.7 %<sup>2</sup>, has a significant influence on the thermodilatometric and elastic behavior of the samples. The  $\alpha \rightarrow \beta$  transition of quartz occurs together with the dehydroxylation of kaolinite in samples S400, S500 and S600. The relationship between Young's modulus and the temperature of S400 and S500 shows a small sharp minimum similar to pure polycrystalline quartz and sandstone.<sup>27,28</sup> The rapid increase in the thermal expansion and the change in the sign of Poisson's ratio lead to the formation of stress at the grain boundaries.<sup>8,29</sup> Young's modulus of samples S400 and S500 is weak and close to Young's modulus of the green samples. The porosity of S400 and S500 is relatively high reaching ≈35 % as estimated from the bulk density of the sample prefired at 400 °C (1.7 g·cm<sup>-3</sup>) and densities of kaolinite (2.5 g·cm<sup>-3</sup>), quartz (2.65 g·cm<sup>-3</sup>) and feldspar (2.6 g·cm<sup>-3</sup>). Therefore, the quartz grains can expand almost freely and do not significantly influence their neighboring kaolinite and feldspar crystals.

A different situation is noted for samples S600–S1200 (**Figures 8, 9 and 10**) where Young's modulus steeply increases over the temperature interval, in which the  $\alpha \rightarrow \beta$  transition of quartz occurs. We met this phenomenon in our previous works<sup>2,5</sup> and in the paper written by A. P. N. de Oliveira et al.<sup>3</sup> where samples fired at temperatures sufficient for forming the glassy phase were measured. The quartz grains are not free here since they are encapsulated by the glassy phase. The quartz grains increase their volume more intensely than the glassy phase. Thus, the quartz grains generate a compressive stress in their close surroundings. Since many quartz grains have circumferential microcracks around them,<sup>3,30,31</sup> the stress has a healing effect, leading to an increase in Young's modulus. Such a situation can be expected for samples S1100 and S1200. But samples S600–S1000 that do not contain the glassy phase, also show a steep increase in Young's modulus caused by the  $\alpha \rightarrow \beta$  transition of quartz. Consequently, the presence of

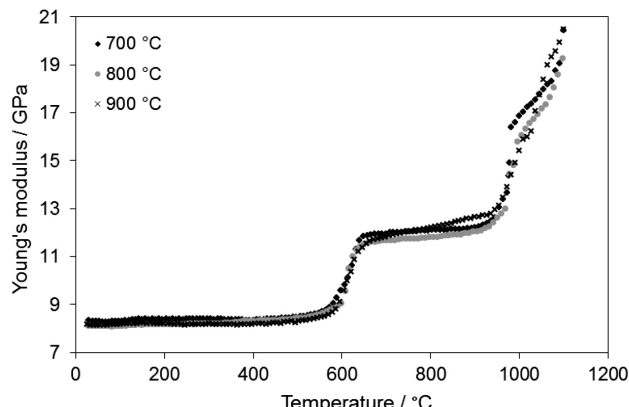


**Figure 9:** Young's modulus of quartz-porcelain samples prefired at (700, 800 and 900) °C

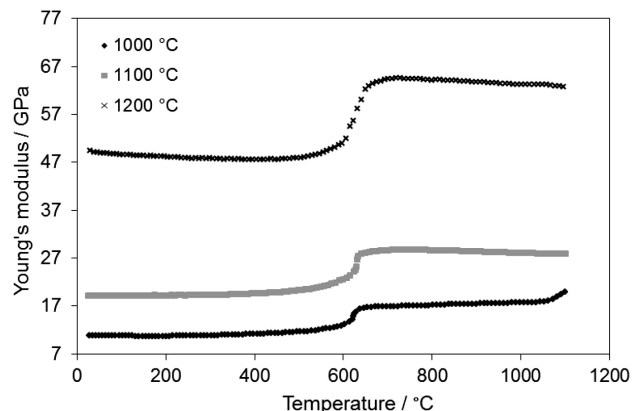


**Figure 10:** Young's modulus of quartz-porcelain samples prefired at (1000, 1100 and 1200) °C

microcracks and tiny pores between the quartz grains and the crystals of metakaolinite and feldspar can be presumed. These microcracks originate from the cooling stage of the previous prefiring.

The microstructure of these samples is similar to that shown in **Figure 11** where the partially sintered mixture of the metakaolinite/Al-Si spinel crystals and grains of quartz and feldspar as well as pores are visible. The presumed microcracks and tiny pores in the close vicinity of the quartz grains can be healed during an intensive thermal expansion of the quartz grains when the sample is heated above 600 °C. The heights of the steps of Young's modulus are different (**Figures 8, 9 and 10**) following the rule "the higher the temperature of preheating, the higher is the step of Young's modulus" or, in other words, "the more developed the solid-state sintering, the higher is the step of Young's modulus". This is well demonstrated in **Table 2** where the initial Young's modulus,  $E(20$  °C), the final Young's modulus

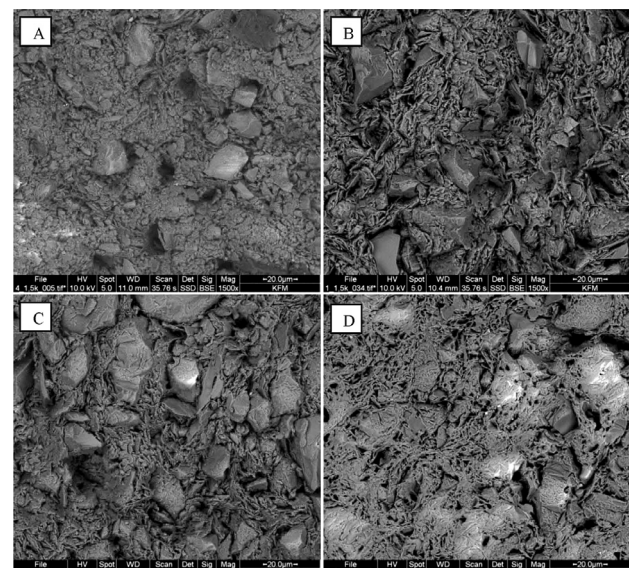


**Figure 11:** SEM pictures of the samples prefired at: a) 400 °C, b) 800 °C, c) 1100 °C and d) 1200 °C

**Table 2:** Initial (at 25 °C) and final (at 1100 °C) Young's modulus and the difference between its values before and after the transition of quartz depending on the prefiring temperature

<i>t</i> / °C	400	500	600	700	800	900	1000	1100	1200
<i>E</i> (25 °C) / GPa	10.3	10.9	9.2	8.3	8.1	8.2	10.8	19.1	49.4
<i>E</i> (1100 °C) / GPa	20.5	20.8	20.8	20.3	19.9	20.4	19.9	27.8	62.7
$\Delta E$ / GPa	—	—	2.5	3.5	3.5	3.5	4.8	8.1	16.6

after the second firing, *E*(1100 °C), and the difference between Young's modulus before and after the  $\alpha \rightarrow \beta$  transition of quartz,  $\Delta E$ , are given. The influence of the  $\alpha \rightarrow \beta$  transition of quartz is clearly visible for all the dehydroxylated samples (S600–S1200) and it is especially strong for S1000, S1100 and S1200 where intensive sintering took place. The low initial values as well as the final values of Young's modulus for S400–S900 are explainable with high porosity and low level of sintering.

The initial values of Young's modulus that are equal to its final values after the prefiring of samples S400–S1000 vary between 8 GPa and 11 GPa, which is also a consequence of the low value of Young's modulus during the prefiring of the green samples over the interval of 20–950 °C when Young's modulus does not exceed 13 GPa.<sup>22</sup> The initial values of Young's modulus for samples S1100 and S1200 are higher, 19 GPa and 49.5 GPa, which is related to the sintering.

We determine the effective value of Young's modulus, which is a combination of Young's modulus of quartz, feldspar and metakaolinite. Only one of them, Young's modulus of quartz, changes rapidly from  $E_{\alpha\text{-quartz}} = 90$  GPa to  $E_{\beta\text{-quartz}} = 110$  GPa, passing through a sharp minimum,<sup>28,32</sup> thus providing an explanation for the steep increase of Young's modulus in the interval of the  $\alpha \rightarrow \beta$  transition of quartz. Similar results were also obtained for fired porcelain tiles.<sup>3</sup>

After a decrease in the  $\alpha \rightarrow \beta$  transition of quartz, Young's modulus of samples S400, S500 and S600 shows a moderate increase due to the solid-state sintering up to  $\approx 950$  °C when the metakaolinite lattice collapses and a new phase (Al-Si spinel) is formed.<sup>33</sup> Its density is higher than that of metakaolinite; therefore, a steep increase in Young's modulus is observed above this temperature. The next process in the samples is crystallization of mullite from spinel above 1050 °C, which is also connected with a significant densification.<sup>20</sup> This is well reflected in Young's modulus of sample S1000 and in the weak indication of samples S400–S900.

The relationships between Young's modulus and the temperature of samples S1100 and S1200 is influenced by the presence of the glassy phase, and the increase in Young's modulus is caused by the closing of the circumferential cracks around the quartz grains.

## 4 CONCLUSIONS

Green cylindrical samples (50 w% of kaolin, 25 w% of quartz and 25 w% of feldspar) were extruded from a

wet plastic mixture. After free drying, the samples were prefired up to 400–1200 °C and then fired up to 1100 °C. Using TG, TDA and D-TMA, the following results and conclusions were obtained for the second firing:

The samples prefired up to 400 °C and 500 °C showed a significant influence of the release of the physically bound water on Young's modulus, which increased by  $\approx 25$  % and 6.5 %, respectively, between room temperature and 200 °C.

The samples prefired up to 400 °C and 500 °C were affected by the  $\alpha \rightarrow \beta$  transition of quartz only to a small extent.

In the samples prefired at temperatures above 500 °C, the  $\alpha \rightarrow \beta$  transition of quartz governed Young's modulus in the interval of 500–700 °C. Young's modulus increased from 29 % to 40 % for the samples prefired at 600–1200 °C due to the closing of the cracks and tiny pores located around the quartz grains. Consequently, the presence of the glassy phase is not necessary for the steep increase in Young's modulus in the  $\alpha \rightarrow \beta$  transition of quartz.

Above 800 °C, solid-phase sintering as well as the formation of Al-Si spinel ( $\sim 950$ –980 °C) and crystallization of mullite (above 1050 °C) increased Young's modulus.

## Acknowledgments

This work was supported by the grants VEGA 1/0425/19 from the Ministry of Education of the Slovak Republic and by RVO: 11000. Authors also wish to thank the Ceramic plant PPC Čab, a.s., for providing green samples.

## 5 REFERENCES

- 1 A. de Noni, D. Hotza, V. C. Soler, E. S. Vilches, Influence of composition in mechanical behaviour of porcelain tile, Part II: Mechanical properties and microscopical residual stress, Mater. Sci. Eng. A – Struct. Mater. Prop. Microstruct. Process., 527 (2010) 7–8, 1736–1743, doi:10.1016/j.msea.2009.10.060
- 2 I. Štubňa, A. Trník, L. Vozár, Thermomechanical analysis of quartz porcelain in temperature cycles, Ceram. Int., 33 (2007) 7, 1287–1291, doi:10.1016/j.ceramint.2006.04.024
- 3 A. P. N. de Oliveira, E. S. Vilches, V. C. Soler, F. A. G. Villegas, Relationship between Young's modulus and temperature in porcelain tiles, J. Eur. Ceram. Soc., 32 (2012) 11, 2853–2858, doi:10.1016/j.jeurceramsoc.2011.09.019
- 4 I. Štubňa, P. Šín, P. A. Trník, R. Podoba, L. Vozár, Development of Young's modulus of the green alumina porcelain raw mixture, J. Aust. Ceram. Soc., 50 (2014) 2, 36–42

- <sup>5</sup> A. Trník, I. Štubňa, G. Varga, M. Keppert, P. Bačík, Structural and thermomechanical properties of stove tile ceramics, *Mater. Sci.-Medzg.*, 19 (2013) 4, 461–464, doi:10.5755/j01.ms.19.4.2916
- <sup>6</sup> M. Jankula, T. Húlan, I. Štubňa, J. Ondruška, R. Podoba, P. Šín, B. Bačík, A. Trník, The influence of heat on elastic properties of illitic clay Radobica, *J. Ceram. Soc. Jpn.*, 123 (2015) 1441, 874–879, doi:10.2109/jcersj2.123.874
- <sup>7</sup> V. Hanykýř, J. Kutzendorfer, *Technology of Ceramics*, Silis Praha, Praha 2008
- <sup>8</sup> W. Pabst, E. Gregorová, J. Kutzendorfer, Elastic anomalies in tridymite and cristobalite-based silica materials, *Ceram. Int.*, 40 (2014) 3, 4207–4211, doi:10.1016/j.ceramint.2013.08.079
- <sup>9</sup> I. Štubňa, A. Trník, R. Podoba, J. Ondruška, L. Vozár, The influence of thermal expansion and mass loss on the Young's modulus of ceramics during firing, *Int. J. Thermophys.*, 35 (2014) 9–10, 1879–1887, doi:10.1007/s10765-012-1366-y
- <sup>10</sup> I. Štubňa, A. Trník, L. Vozár, Determination of Young's modulus of ceramics from flexural vibration at elevated temperatures, *Acta Acust. United Acust.*, 97 (2011) 1, 1–7, doi:10.3813/AAA.918380
- <sup>11</sup> Y. H. Cuff, *Ceramic technology for potters and sculptors*, University of Pennsylvania Press, Philadelphia, 1996
- <sup>12</sup> B. Plešingerová, M. Klapáč, M. Kovalčková, Moisture expansion of porous biscuit bodies – reason of glaze cracking, *Ceram.Silik.*, 46 (2002) 4, 159–165
- <sup>13</sup> A. Kara, An investigation into bloating behaviour of bone China body during biscuit firing, *Key Eng. Mater.*, 264–268 (2004), 1717–1720, doi:10.4028/www.scientific.net/KEM.264-268.1717
- <sup>14</sup> A. Kara, R. Stevens, Interactions between an ABS type leadless glaze and a biscuit fired bone china body during glost firing. Part I: Preparation of experimental phases, *J. Eur. Ceram. Soc.*, 22 (2002) 7, 1095–1102, doi:10.1016/S0955-2219(01)00419-8
- <sup>15</sup> A. Kara, R. Stevens, Interactions between an ABS type leadless glaze and a biscuit fired bone china body during glost firing. Part II: Preparation of experimental phases, *J. Eur. Ceram. Soc.*, 22 (2002) 7, 1103–1112, doi:10.1016/S0955-2219(01)00420-4
- <sup>16</sup> A. Kara, R. Stevens, Interactions between an ABS type leadless glaze and a biscuit fired bone china body during glost firing. Part III: Effect of glassy matrix phase, *J. Eur. Ceram. Soc.*, 23 (2003) 10, 1617–1628, doi:10.1016/S0955-2219(02)00403-X
- <sup>17</sup> M. Jankula, P. Šín, R. Podoba, J. Ondruška, Typical problems in push-rod dilatometry analysis, *Építőanyag*, 65 (2013) 1, 11–14, doi:10.14382/epitoanyag-jsbcm.2013.3
- <sup>18</sup> R. Podoba, A. Trník, L. Podobný, Upgrading of TGA/DTA analyzer Derivatograph, *Építőanyag*, 64 (2012) 1–2, 28–29, doi:10.14382/epitoanyag-jsbcm.2012.5
- <sup>19</sup> ASTM C848-88:2016 Standard test method for Young's modulus, shear modulus and Poisson's ratio for ceramic whitewares by resonance, ASTM International, West Conshohocken USA
- <sup>20</sup> P. Ptáček, M. Křečková, F. Šoukal, T. Opravil, J. Havlica, J. Brandstetr, The kinetics and mechanism of kaolin powder sintering I. The dilatometric CRH study of sinter-crystallization of mullite and cristobalite, *Powder Technol.*, 232 (2012), 24–30, doi:10.1016/j.powtec.2012.07.060
- <sup>21</sup> F. Freund, Kaolinite-metakaolinite, a model of a solid with extremely high lattice defect concentration, *Ber. Deutsche Keram. Ges.*, 44 (1967) 1, 5–13
- <sup>22</sup> I. Štubňa, F. Chmelík, A. Trník, P. Šín, Acoustic study of quartz porcelain during heating up to 1150 °C, *Ceram. Int.*, 38 (2012) 8, 6919–6922, doi:10.1016/j.ceramint.2012.05.021
- <sup>23</sup> I. Štubňa, T. Kozík, Permeability of the electroceramics to gas and its dependence on the firing temperature, *Ceram. Int.*, 23 (1997) 3, 247–249, doi:10.1016/S0272-8842(96)00034-X
- <sup>24</sup> F. H. Norton, *Fine Ceramics: Technology and Applications*, McGraw-Hill Book Co., New York 1970
- <sup>25</sup> I. Štubňa, P. Šín, A. Trník, R. Veinthal, Mechanical properties of kaolin during heating, *Key Eng. Mater.*, 527 (2013), 14–19, doi:10.4028/www.scientific.net/KEM.527.14
- <sup>26</sup> G. Varga, The structure of kaolinite and metakaolinite, *Építőanyag*, 59 (2007) 1, 6–9, doi:10.14382/epitoanyag-jsbcm.2007.2
- <sup>27</sup> Z. W. Peng, S. A. T. Redfern, Mechanical properties of quartz at the  $\alpha \rightarrow \beta$  phase transition: Implications for tectonic and seismic anomalies, *Geochem. Geophys. Geosyst.*, 14 (2013) 1, 18–28, doi:10.1029/2012GC004482
- <sup>28</sup> W. Pabst, E. Gregorová, Elastic properties of silica polymorphs - A review, *Ceram.-Silik.*, 57 (2013) 3, 167–184
- <sup>29</sup> A. N. Nikitin, G. V. Markova, A. M. Balagurov, R. N. Vasin, O. V. Alekseeva, Investigation of the structure and properties of quartz in the  $\alpha$ - $\beta$  transition range by neutron diffraction and mechanical spectroscopy, *Crystallogr. Rep.*, 52 (2007) 3, 428–435, doi:10.1134/S1063774507030145
- <sup>30</sup> J. Liebermann, About the important correlation between microstructure properties and product quality of strength-stressed high-voltage insulators, Part 1, *Interceram.*, 53 (2004) 4, 238–241
- <sup>31</sup> J. Liebermann, About the important correlation between microstructure properties and product quality of strength-stressed high voltage insulators - rules and reference values for manufacturers and users, Part 2, *Interceram.*, 54 (2005) 1, 16–21
- <sup>32</sup> G. N. Greaves, A. L. Greer, R. S. Lakes, T. Rouxel, Poisson's ratio and modern materials, *Nat. Mater.*, 10 (2011) 11, 823–837, doi:10.1038/NMAT3134
- <sup>33</sup> P. Ptáček, F. Šoukal, T. Opravil, N. Nosková, J. Havlica, J. Brandstetr, Mid-infrared spectroscopic study of crystallization of cubic spinel phase from metakaolin, *J. Solid State Chem.*, 184 (2011) 10, 2661–2667, doi:10.1016/j.jssc.2011.07.038